Operation of the RF Controls in the CEBAF Injector *

S. N. Simrock, J. A. Fugitt, J. C. Hovater, G. A. Krafft, C. K. Sinclair

Continuous Electron Beam Accelerator Facility
12000 Jefferson Avenue
Newport News, Virginia 23606

Abstract

The CEBAF injector has produced its first relativistic beam with two superconducting cavities. Six RF control modules are used to control amplitude and phase in the chopper cavities, the buncher, the capture section, and the two superconducting cavities. In this paper the required stability and actual performance of the modules are discussed. For the superconducting cavity control, performance is consistent with energy stability of $\approx 10^{-4}$.

Introduction

The main goal of the injector test underway is to produce chopped and bunched CW beam at 500 keV and to accelerate the beam to 5 MeV with superconducting cavities. The test will verify the design characteristics of the RF control system with beam and will lead to a final design of the linac RF controls. At the end of this year the injector will be installed at its final location in the accelerator tunnel.

RF Control System

Stringent RF control is needed at CEBAF under various operating conditions such as different field gradients and beam loads. A schematic diagram of the RF control system for the injector test is shown in Figure 1. Six control modules are used to control amplitude and phase in the two chopper resonators, the buncher, the capture section and two standard superconducting cavities.

One of the 338 RF control channels for the superconducting cavities, described elsewhere, [1,2,3] is shown in Figure 2. The essential component is the standard RF control module which

itself is divided into four separate sections. They are a RF converter, an IF board, an analog board and a digital section. The variable gain stages on the analog board allow optimization of the frequency response in the feedback loops for phase and amplitude. A typical frequency response is shown in Figure 3. Variable frequency response is necessary to minimize residual errors since the actual microphonic noise sources in the tunnel are not well known. The operator has control over the broadband gain from 20 to 60 dB and additional low frequency gain up to 30 dB. The rolloff frequency for the low frequency boost is adjustable from 1 Hz to 200 Hz. Including the cavity, unity gain is reached at up to 100 kHz with a phase margin of 60 degrees. Variations of the gain characteristics are also used to adjust for differences in the loaded Q of the cavities.

The RF drive to the chopper and buncher cavities is provided by 25 W class 'C' amplifiers. The amplitude control section of the standard RF module required modification. The level modulator in the IF section is kept at a constant bias, providing sufficient drive for the 25 W amplifier. The amplified amplitude error signal feeds the input of a modulator which provides the DC power for the 25 W amplifier.

The high power amplifier for the capture section uses two 5 kW klystrons to provide 9.5 kW drive with some margin for amplitude control. Preamplifiers provide sufficient gain to operate the capture section with the drive of a RF control module. Low pass filters with 100 Hz rolloff had to be added in the control loops to achieve the same overall frequency response as for the SC cavities.

The capture section needs to be temperature stabilized to $\pm 0.1°$ F. A digital PID controller is implemented within the TACL system [4]. It uses the phase difference between drive and
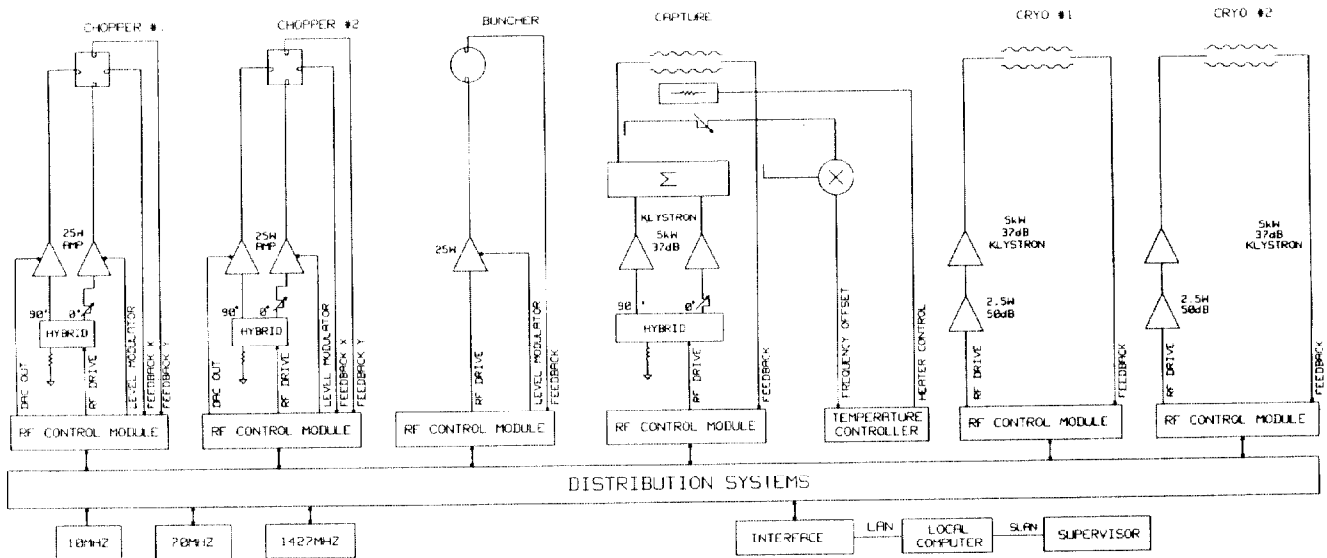

Figure 1. RF control system used in the injector test.

probe signals as a temperature error signal and a water servo-valve serves as the controller. In equilibrium, the heating power comes from the RF (9.5 kW). A 5 kW electrical heater provides the power for initial warmup.
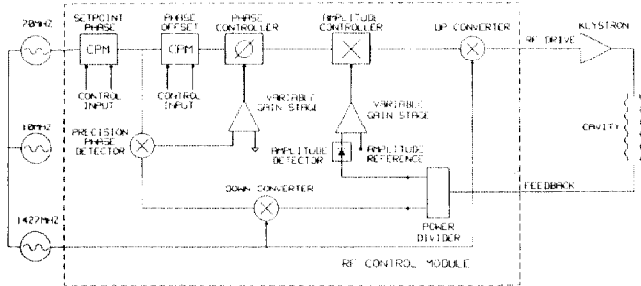

Figure 2. Simplified schematic of a standard CEBAF RF control module.

Performance of RF Controls

Requirements

The performance of the RF controls is measured by the residual amplitude and phase fluctuation in the cavities. Noise sources are microphonic noise, beam induced noise (severe in pulsed mode operation) and system intrinsic noise such as noise from the master oscillator, from the low level amplifiers in the feedback loops, or from the klystron. Table 1 summarizes the requirements for amplitude and phase regulation to achieve $\Delta E/E$ of 10^{-4} in the final linac beam.

Table 1
Error Tolerances for the Fields in the Cavities

Cavity	Amplitude Error	Phase Error [°]	
SC cavity	$\pm 2 \times 10^{-5}$	± 0.2	correlated
SC cavity	$\pm 4 \times 10^{-4}$	± 0.5	uncorrelated
Chopper	$\pm 1 \times 10^{-2}$	± 0.2	vertical
Chopper	$\pm 1 \times 10^{-2}$	± 0.2	horizontal
Buncher	$\pm 1 \times 10^{-2}$	± 0.1	
Capture	$\pm 5 \times 10^{-4}$	± 0.2	

Superconducting Cavities

The dominating noise sources in the unlocked (open loop) mode are phase and amplitude errors caused by mechanical vibrations of the cavity. A typical phase error signal for the two SC cavities is shown in Figure 4. The signal has peak to peak fluctuations of up to 20°, and the corresponding amplitude fluctuations are up to 6%. The noise of two cavities in the same cryounit is not completely correlated since the mechanical resonance frequencies are different and the excitation shows a broad band of frequencies up to a few hundred Hz. In the locked case, a noise reduction of 90 dB for frequencies below 100 Hz was achieved. For example, Figure 5 shows the amplitude noise spectrum for the regulated and unregulated case. The low frequency gain was set to 30 dB, the rolloff frequency to 200 Hz, and the broadband gain to 60 dB. Below 1 kHz the residual noise is dominated by 60 Hz, at the $\pm 7 \times 10^{-5}$ level. This level is three times greater than the correlated error limit. This noise will be reduced by avoiding ground loops, and its effects can be minimized by choosing different line phases for the control modules.
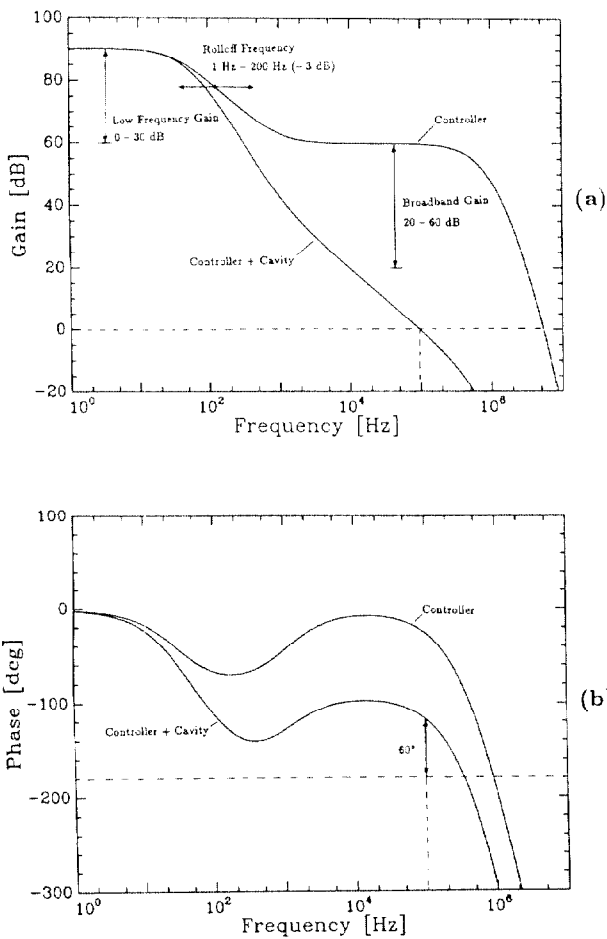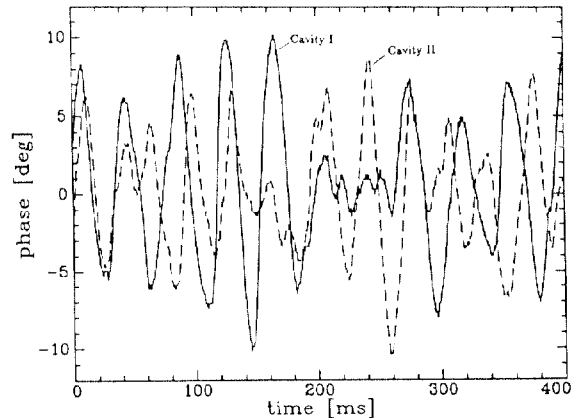

Figure 3. Frequency response (a) magnitude and (b) phase of gain stages in amplitude and phase controller. Broadband gain is variable from 20 – 60 dB, low frequency gain from 0 – 30 dB and rolloff frequency from 1 Hz to 200 Hz.

Figure 4. Phase noise in the two superconducting cavities of one cryounit. Data taken at same time shows correlation of signals.
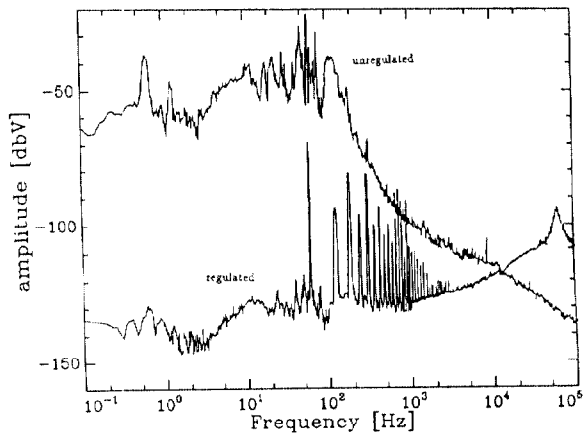
Figure 5. Spectrum of gradient fluctuations in regulated and unregulated mode.

Table 2 lists the amplitude and phase errors for the regulated cavity without beam. The broadband noise for frequencies above 1 kHz is about twice as high as the noise below 1 kHz. It should be noted that for the amplitude noise measurements, an external amplitude detector was used to detect the actual noise in the cavity. This is necessary since the amplitude detector in the feedback loop creates 60 Hz noise which cannot be measured in the loop.

Table 2
Measured Errors for the Fields in the SC Cavities

Bandwidth [Hz]	Amplitude Error	Phase Error [°]
10^0	$\pm 1.1 \times 10^{-5}$	$\pm 2.2 \times 10^{-3}$
10^1	$\pm 2.2 \times 10^{-5}$	$\pm 2.3 \times 10^{-3}$
10^2	$\pm 6.9 \times 10^{-5}$	$\pm 6.0 \times 10^{-3}$
10^3	$\pm 8.1 \times 10^{-5}$	$\pm 9.1 \times 10^{-3}$
10^4	$\pm 1.1 \times 10^{-4}$	$\pm 1.4 \times 10^{-2}$
10^5	$\pm 1.4 \times 10^{-4}$	$\pm 3.2 \times 10^{-2}$
10^6	$\pm 1.5 \times 10^{-4}$	

Capture Section

The phase and amplitude noise in the capture section are dominated by 720 Hz (and harmonics) from the klystron power supply. Low frequency drifts are compensated with the temperature controller. To reduce the broadband noise in the capture section to acceptable levels, the frequency response of the control module will be modified.

Table 3
Measured Errors for the Fields in the Capture Section

Bandwidth [Hz]	Amplitude Error	Phase Error [°]
10^2	$\pm 2.2 \times 10^{-5}$	$\pm 4.0 \times 10^{-3}$
10^3	$\pm 5.5 \times 10^{-5}$	$\pm 3.6 \times 10^{-2}$
10^4	$\pm 3.3 \times 10^{-4}$	$\pm 1.8 \times 10^{-1}$
10^5	$\pm 8.7 \times 10^{-4}$	$\pm 2.2 \times 10^{-1}$
10^6	$\pm 9.5 \times 10^{-4}$	$\pm 2.4 \times 10^{-1}$

Chopper and Buncher

The phase and amplitude noise in the chopper and buncher resonators are dominated by 60 Hz and broadband noise from the amplitude detector and phase reference. Slow frequency drifts are compensated with the temperature controller.

Table 4
Measured Errors for the Fields in the Chopper Cavities and the Buncher Cavity

Bandwidth [Hz]	Amplitude Error	Phase Error [°]
10^2	$\pm 6.7 \times 10^{-5}$	$\pm 6.5 \times 10^{-3}$
10^3	$\pm 1.1 \times 10^{-4}$	$\pm 4.8 \times 10^{-2}$
10^4	$\pm 4.7 \times 10^{-4}$	$\pm 9.5 \times 10^{-2}$
10^5	$\pm 1.4 \times 10^{-3}$	$\pm 1.4 \times 10^{-1}$
10^6	$\pm 1.5 \times 10^{-3}$	$\pm 1.6 \times 10^{-1}$

Conclusion

The recent tests on the RF control system at CEBAF have shown that it is possible to control phase in the SC cavities to $\ll \pm 0.2°$ and the amplitude to $< \pm 4 \times 10^{-4}$. The microphonic noise in different cavities is unlikely to be correlated and it is corrected adequately. The correlated 60 Hz noise is $\pm 7 \times 10^{-5}$, greater than the error limit. This noise will be reduced by avoiding ground loops, and its effects can be minimized by different line phases. The regulation of the field in the chopper and buncher cavities is adequate. The amplitude control for the capture section is close to the requirements and the control module will be modified to reduce the noise to tolerable levels. Overall, the RF controls for the CEBAF injector have been in operation for more than two months without failure.

Acknowledgement

References

1. S. Simrock, C. Hovater, S. Jones and J. Fugitt, Proceedings of the 1989 Particle Accelerator Conference, Chicago, Illinois, March 20–23, 1989, p. 1885.

2. C. Hovater and J. Fugitt, 1988 Linear Accelerator Conference Proceedings, Newport News, Virginia, October 3–7, 1988, p. 412.

3. I. Ashkenazi and G. Lahti, Proceedings of the 1989 Particle Accelerator Conference, Chicago, Illinois, March 20–23, 1989, p. 1861.

4. R. Bork, 1987 IEEE Particle Accelerator Conference, Washington, D.C., March 16–19, 1987, p. 523.